Pseudo-stationary capacitance and conductance for open air artificially generated long electrical arcs considering arc elongation

A. Garcia, M. C. Tavares

Abstract—**The major part of disturbs in electrical systems occurs in transmission lines. These disturbs are in most cases single-phase and transitory and mainly caused by atmospheric electrical discharges. In this paper, the voltage-current cross relation characteristic of the secondary arc was investigated using open air experimental data. With more than 400 artificially generated long electrical arcs, a methodology to calculate the stationary secondary arc conductance and capacitance is presented, alongside with the capacitive and conductive values for several arc currents.**

Keywords: **Secondary arc, modeling, single-phase fault, experimental data, conductance values, capacitance values.**

I. INTRODUCTION

THE majority of disturbs in electrical systems occurs in transmission lines. These disturbs are in most cases single-phase and non-permanent, representing 80% to 90% of the total number of faults [1], [2], which is even more common in high voltage and extra high voltage (EHV) transmission lines. Due to its continental dimension, Brazil has a large number of EHV lines.

When a fault occurs in the power system, an electrical arc appears in the fault location. For instance, sometimes the fault currents and temperatures are very high, not only the assets in the fault location are damaged, but also other nearby equipment are damaged. Therefore, it is of great importance to investigate the electrical arc phenomena to be able to rapidly recover from a fault, to identify its causes and to prevent future faults.

Single-phase faults are mainly caused by atmospheric electrical discharges. When these discharges strike the transmission lines, they can overcome the insulation distance, ionizing the air, creating a low impedance path allowing current flow. This path is called an electrical arc and may remain indefinitely as long as a high current flows.

When the transmission lines are affected by electrical arcs the protection systems should act, so that the arc is quickly eliminated, maintaining system stability and restoring normal power supply. To eliminate transient single-phase faults involving electrical arcs, single phase auto-reclosure (SPAR) is the most recommended maneuver.

In the SPAR only the faulty phase circuit-breakers open by a predetermined time interval, called dead time. Typical dead time values are within 0.5 seconds to 1 second, which ensures a high probability of secondary arc extinction. After this time the line is reconnected. Throughout this maneuver the other phases keep transmitting energy [3], allowing a power flow around 54% of total power on simple circuit lines and 75% on double circuit lines. This feature gives SPAR some advantages in comparison with the three-phase auto-reclosure maneuver, promoting a much smaller disturbance to the power system, as described below:

- Improved stability in transient state;
- Reduction of switching overvoltages;
- Reduction of generators rotors torsional oscillations;
- Uninterrupted power transmission.

The SPAR will be more advantageous only if it has a high rate of success in extinguishing the secondary arc, because if it fails, the three-phase maneuver should be used. The success of this operation is directly related to the secondary arc behavior during the SPAR. The secondary arc is the electric arc following a single-phase to ground fault associated to a primary arc after faulty phase opening at both terminals, maintaining connected the other line phases.

This secondary arc may be sustained, maintaining the short circuit arc channel ionized by the inductive and capacitive coupling effect between phases and other possible phase interactions, e.g. through line shunt reactors. The success of the SPAR relies on the secondary arc extinction during the dead time, which in turn must be minimized in order to reduce disturbances in the system [4]–[6].

The secondary arc behavior is very complex, influenced by a variety of parameters. The extinction time of the secondary arc depends on such parameters, which include: electric network-arc interaction, line compensation levels, transmission line length, fault location occurrence along the line, secondary arc current amplitude, line nominal voltage and random weather related variables such as wind, humidity and temperature [5], [7], [8].

One of the main concerns in power systems is the correct modeling of the components in frequency bands compatible with the phenomena under study. For studies of the transitory

arc behavior, a more detailed representation of the involved equipment and phenomena is necessary, taking into account the behavior as a function of the involved frequency and nonlinearities.

Thus the correct mathematical representation of the secondary arc is needed for a better network operation and to adjust the protection.

In the next sections new results are presented, specifically the voltage-current cross relation characteristic of long secondary arc generated in an open air experiment. A methodology to obtain the stationary arc conductance and capacitance is presented, being applied to more than 400 electrical arcs. The arc current range varies from $15 \ A_{rms}$ to $3000 \ A_{rms}$.

II. EXPERIMENTS

As the secondary arc extinction depends on various factors, it is important to study these phenomena as close as possible to real conditions in the power system.

In 2003, an important research project in Brazil was initiated to evaluate and improve the performance of single-phase autoreclosure in transmission lines [9], [10]. The main objective of that research project was to acquire and validate a robust model of the secondary arc in free air, enabling the simulation of interaction between the arc and network as well as the SPAR success (or failure) determination.

A. High Power Laboratory Experiments

The data used in this paper was produced through field tests conducted by the CEPEL High Power Laboratory in Adrianópolis, Brazil, from 2004 to 2010 [9], [10]. In this laboratory an experimental 500 kV transmission line section was installed, shown in Fig. 1, which represents actual tower transmission conditions.
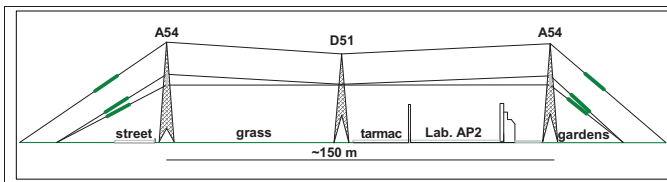

Fig. 1: Testing setup formed by three 500 kV tower structures.

The section is formed by three transmission towers, one anchor tower positioned between two suspension towers, and all the other elements such as insulator strings, shield rings, phase conductors and ground wires.

The tests consisted of generating the electrical arc by imposing a sustained current of $60 Hz$ for 1 second. In the tests arc currents of up to $10,000 \ A_{rms}$ were imposed. This paper presents the analysis of tests with current levels of $15 \ A_{rms}$, $20 \ A_{rms}$, $30 \ A_{rms}$, $50 \ A_{rms}$, $60 \ A_{rms}$, $100 \ A_{rms}$, $150 \ A_{rms}$, $200 \ A_{rms}$, $300 \ A_{rms}$, $500 \ A_{rms}$, $1000 \ A_{rms}$ and $3000 \ A_{rms}$.

The arc is formed between the top point of the insulator string, connected to the tower structure, which is grounded, and the bottom point of the string, connected to the phase, with

Fig. 2: Picture take during a field test.

the use of a fuse wire connected in parallel to the insulator string which is $4.05 \ m$ in length as shown in Fig. 2.

The current passing through this wire enables the arc ignition and then the wire vaporizes. After 1 s of arc ignition the sustained current is interrupted (it does not self-extinguish). I-shaped insulator strings were used in the vast majority of the tests analyzed in this study, but some V-shaped strings were also used.

To apply the current to the system, an external generator is used, supplying a constant rms value of $60 \ Hz$ current directly to the phase in which the fault is simulated. This would represent a secondary arc maintained by capacitive and inductive coupling with the healthy phases in a transmission line which have basically fundamental frequency voltage and current.

The samples are acquired and stored by a system developed by CEPEL. This acquisition system is currently capable of processing 20 million samples per second through 4 independent channels, registering the voltages at each arc terminal, the sustained current ($60 \ Hz$) and impulse currents (not used in this study).

Using two cameras (Fig. 3), a visual record of each test was also made, and the meteorological conditions during the test are also recorded, such as temperature, wind speed, humidity and pressure. The objective was to estimate the arc length variation during the experiment [11], [12].
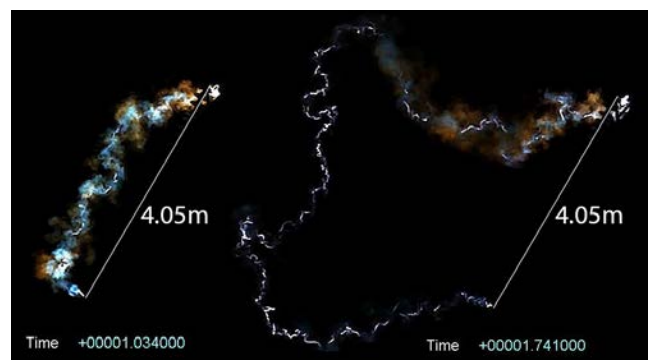

Fig. 3: Images of a $1000 \ A_{rms}$ arc test.

B. System Characteristics

Typical voltage and current values are presented in Fig. 4. In this figure the voltage shown increases over time because of the arc elongation.
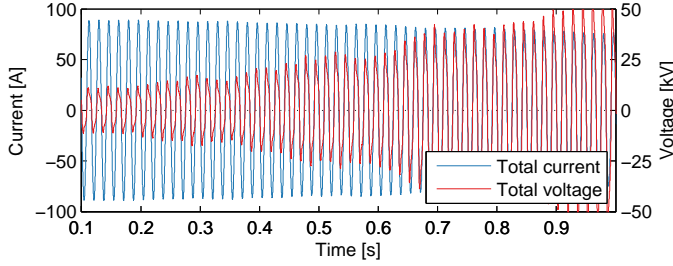

Fig. 4: Voltage and current for 60 A_{rms} arc after filtering.

As shown in Fig. 5, the waveform of the voltage is not similar to the current one. This distorted shape is due to the influence of the harmonics generated by the arc formation, mainly caused by the 3rd and 5th order harmonics [8].
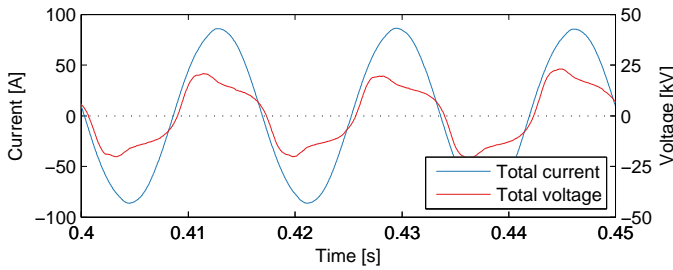

Fig. 5: Voltage and current for 60 A_{rms} arc after filtering.

In Fig. 4 and Fig. 5 the sustained current is shown, being imposed to one of the phases to simulate the secondary arc phenomena that would be generated due to the coupling to the others healthy phases.

The arc voltage-current characteristic is defined by the relationship between the voltage between the arc terminals and the arc current. This waveform, which is similar to a hysteresis, can be observed in Fig. 6, where the data shown is in raw format.

In this figure the arc voltage-current characteristic shown directly from the measurements is defined only by its outer contour and highlights the need for signal processing.

This signal processing may be accomplished either by the use of filters or by a better characterization of the magnitudes involved, i.e., the separation of what actually is related to the phenomena analyzed and what is originated by the experimental process.

In Fig. 5 and Fig. 6 it can be noted that the intersection of voltages and currents does not occur at zero, as is expected for the arc conductive behavior. There is a small displacement in the arc voltage, indicating that there is a capacitive element, which should be also represented.
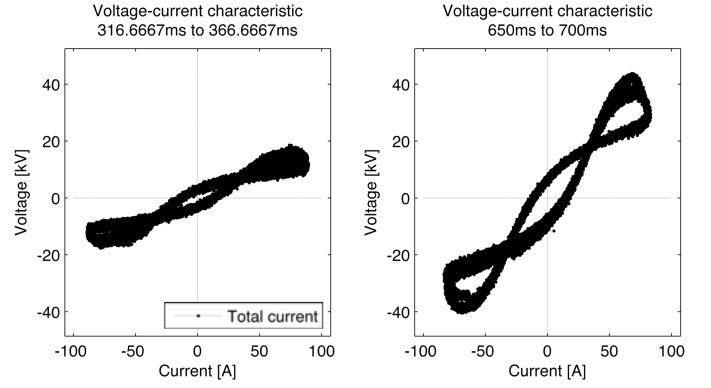

Fig. 6: Secondary arc voltage-current characteristic before filtering.

III. METHODOLOGY

Due to that small capacitive characteristic, the secondary arc current can then be defined as having the following parcels as shown in equation 1: the conductive current and the displacement current, plus the residual current.

$$i(t) = g(t).v_a(t) + c(t)\frac{dv_a(t)}{dt} + i_r(t) \qquad (1)$$

where $i(t)$ is the unidirectional current, $g(t).v_a(t)$ represents the conductive current, $c(t)dv_a(t)/dt$ represents the displacement current and $i_r(t)$ is the residual current that results from measurement noise and system adjustments. The equivalent circuit can be seen in Fig. 7.
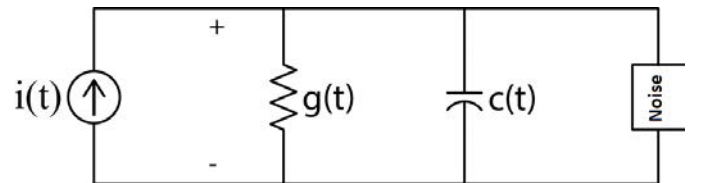

Fig. 7: Equivalent circuit.

Besides the filters for noise attenuation, the conductance current must be calculated, which implies in the subtraction of the unidirectional component current, displacement current, and residual current.

It is worth mentioning that the $c(t)$ portion related to capacitance displacement current refers to the polarization observed between the ends of the insulator string, inherent to the capacitive plasma effect. Additionally the conductance $g(t)$, signal actually modeled, is equivalent to the ionized particles which move inside an electrical field.

A. Filtering and Resample

In order to properly represent the dynamic response of the electrical arc, the signals collected for study were initially sampled at 20 MHz. In this study, as the objective is to treat the quasi-stationary parameters, the data were then resampled to a lower rate, reducing the computational work and the amount of noise present.

For data filtering a FIR filter with linear phase and a high order was needed, as the total decimation factor of data was 2500 times, reducing the sampling frequency to $4\ kHz$, in addition to a zero-phase filtering. A decimation by a factor of 2500 means that, for a sampling frequency of $20\ MHz$ and a zero phase filtering, the first 4000 samples of the signal should be ignored and a sample should be collected, following another 7999 samples should be ignored and another sample should again be collected. And the second part of this procedure should be repeated as many times as it is necessary until the end of the filtered signal.

This step is critical for subsequent calculations, because the incorrect filtering of signals may cause several inconsistencies in the results. A filtering without proper cutoff frequency, especially for cases involving derivative signal calculation, can generate asymptotes and other nonexistent characteristics in the phenomena under study.

Since the data decimation factor is very high, there was a huge computational effort, so the filtering and re-sampling functions were divided into two stages, each one with a decimation factor of 50 times, obtaining at the end the same result that would be obtained with a single stage.

B. Pseudo-Stationary Parameters

The residual current, shown in equation 1, is a random element and can be removed by filtering. The current $i'(t)$ can be used as shown in equation 2.

$$i'(t) = i(t) - i_r(t) \tag{2}$$

Then the next stage is the separation of the conductive current of the electrical arc.

To accomplish this calculation it is first necessary to obtain the values of the capacitance, referring to the displacement current, and the conductance of the arc. Using the trapezoidal integration rule on equation 1, it is obtained:

$$\frac{i'(t) + i'(t - \Delta t)}{2} = G\frac{v_a(t) + v_a(t - \Delta t)}{2} \\ + C\frac{v_a(t) - v_a(t - \Delta t)}{\Delta t} \tag{3}$$

From equation 3 and using three consecutive samples of the signal, an equation system can be created, resulting in the capacitance and conductance of the circuit as shown in equation 4:

$$C = \frac{\Delta t}{2}\frac{(i_2 + i_1)(v_3 + v_2) - (i_3 + i_2)(v_2 + v_1)}{(v_2 - v_1)(v_3 + v_2) - (v_3 - v_2)(v_2 + v_1)} \tag{4a}$$

$$G = \frac{(i_2 + i_1)(v_3 - v_2) - (i_3 + i_2)(v_2 - v_1)}{(v_2 + v_1)(v_3 - v_2) - (v_3 + v_2)(v_2 - v_1)} \tag{4b}$$

where the values of $i'(t_n)$ have been simplified to i_n and $v_a(t_n)$ to v_n.

IV. RESULTS

With the methodology presented in the previous session, after filtering and re-sampling the original data, it was possible to obtain the values of the quasi-stationary conductance and capacitance of the electrical arc. Fig. 8 and Fig. 9 show the values obtained for a $60\ A_{rms}$ test.
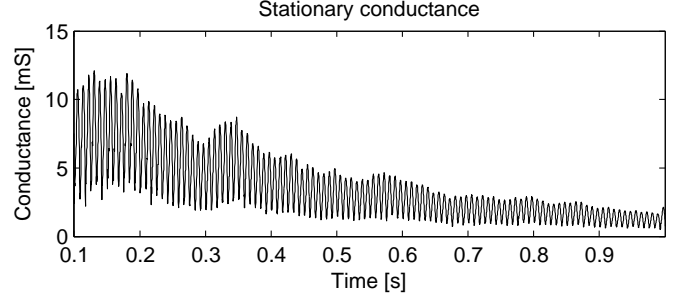

Fig. 8: Conductance obtained for a $60\ A_{rms}$ test.

In Fig. 8 it is shown the arc conductance in each cycle, with higher values for current peaks and lower values for zero crossing current.
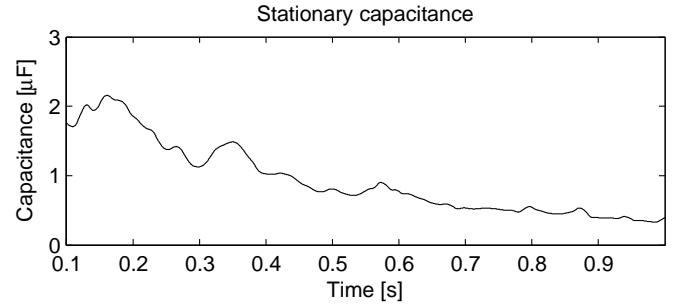

Fig. 9: Capacitance obtained for a $60\ A_{rms}$ test.

In Fig. 8 and Fig. 9 it can be observed that the values of capacitance and conductance decrease along the experiment, whilst the arc voltage increases due to the arc elongation.

After obtaining the conductance and capacitance values, the conduction current and displacement current can be obtained, as proposed in equation 1 and shown in Fig. 10. In Fig. 11 only the conductive current was used to generate the arc voltage-current characteristic. Normally this is the curve presented as the experimental arc result. This characteristic is the one actually used to model the arc.

A. Current Classes

For the same test shown in Fig. 8, Fig. 12 shows in detail the conductance waveform.

As the conductance values vary during the experiment, an average of the conductance per cycle is presented. That means, for each arc experiment the average of the conductance within a cycle is used, repeating the process for each cycle. It can be observed that the conductance varies along the time and this will be analyzed in the following section.
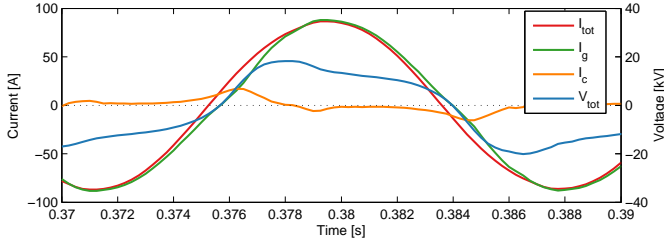
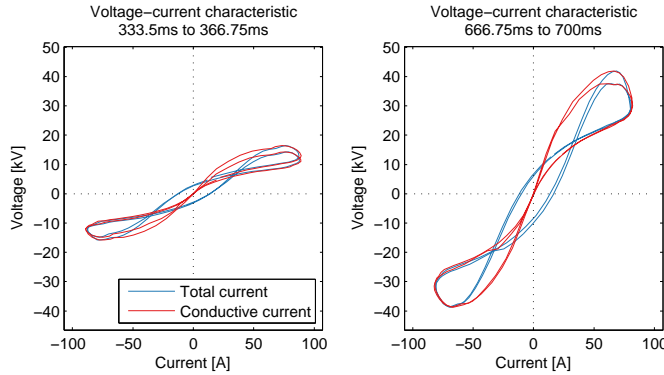Fig. 10: Currents and voltage obtained from a 60 A_{rms} test.

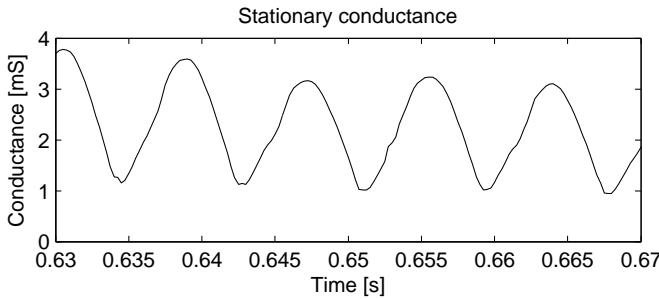Fig. 11: Stationary secondary arc conductance current obtained from a 60 A_{rms} test.

Fig. 12: Arc conductance for 60 A_{rms} from 630 to 670 ms.

In Fig. 13 all the analyzed experiments are presented. This figure shows the conductance and capacitance values for all current classes, where a mean value was obtained for each arc current class.

It can be noted that the behavior of capacitance and conductance are similar for all arc classes, where the values decrease with increasing voltage, which is a response to the electrical arc elongation.

Table I and Fig. 14 show in detail the conductance and capacitance mean values for one single instant, specifically the instant 300 ms. This instant was chosen because it is the former instant where the arc could be considered already stabilized [8] and corresponded to the smallest arc elongation. At this instant these values could be compared with minimum influence of the arc elongation as no arc length was taken into account in this analysis.
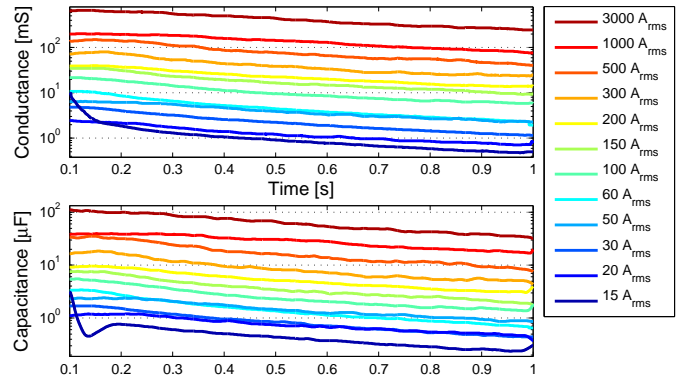

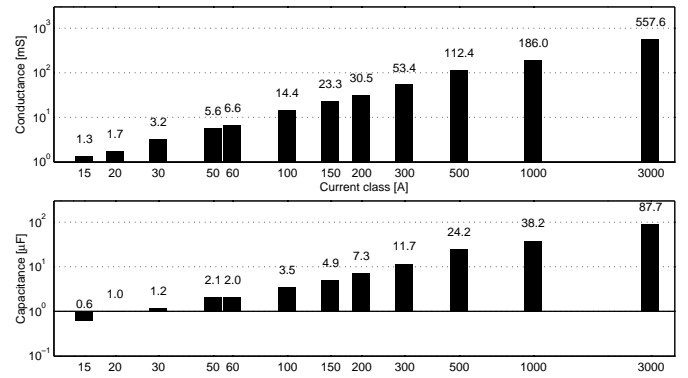Fig. 13: Mean conductance and capacitance values for each arc current class.

Fig. 14: Mean conductance and capacitance values at 300 ms for each arc current class.

TABLE I

Mean and standard deviation of capacitance and conductance for 300 ms.

Current class	Conductance		Capacitance	
	$G(mS)$	$\sigma\ (mS)$	$\overline{C}(\mu F)$	$\sigma\ (\mu F)$
15 A_{rms}	1.30	0.36	0.62	0.40
20 A_{rms}	1.74	0.52	1.05	0.47
30 A_{rms}	3.28	1.01	1.22	0.82
50 A_{rms}	5.57	1.77	2.07	0.63
60 A_{rms}	6.63	1.76	2.11	1.13
100 A_{rms}	14.41	3.01	3.50	0.96
150 A_{rms}	23.28	3.95	4.81	0.86
200 A_{rms}	30.47	5.75	7.15	1.12
300 A_{rms}	53.28	8.85	11.26	1.87
500 A_{rms}	112.18	17.23	23.41	3.86
1000 A_{rms}	186.00	22.98	38.20	8.08
3000 A_{rms}	557.58	124.24	87.71	23.11

In Fig. 14 and Table I it can be seen that both the conductance and capacitance increase with the current rate.

B. In cycle parameter change

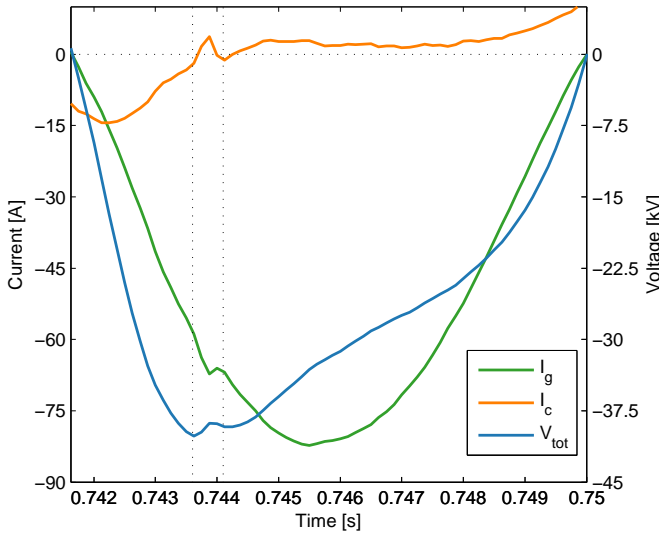In Fig. 15 it can be seen between $743.6\ ms$ and $744.1\ ms$ a rapidly voltage and current change.

Fig. 15: Conductive and capacitive currents and voltage detail for a closing loop occurrence.

This voltage change is due to one or more closing loops occurrence [12]. When a loop closes in the arc path its length has an instante reduction instead of a constant increase. This change affects the pseudo-stationary parameters as can be seen at some points in Fig. 8, Fig. 9 and Fig. 12.

This behavior becomes more clear when the image from the arc are analysed. In the Fig. 16, Fig. 17 and Fig. 18 it can be seen in the regions marked as B and C two loops closing.

Fig. 16, Fig. 17 and Fig. 18 have half cycle difference, and this can be noticed be the circle A, where the brightness level of Fig. 16 and Fig. 18 are around 30 % higher than Fig. 17, representing the minimum, maximum and zero crossing voltage moment.

The constant arc voltage positive and negative cycles do not occur in open-air long arcs due to environmental conditions, specifically due to wind elongating the arc and forming loop that will eventually close in itself, reducing abruptly the arc length. In confined short arcs this variation may be less important. This will make the conductance vary along the time.

V. Conclusions

The SPAR's techniques are of great importance to transmission lines protection systems and their equipment, and the success of this operation is directly related to the secondary arc behavior, which is very complex and influenced by several parameters and external factors.

In this paper a methodology was presented to identify and obtain the parcels that form the arc current. Normally only the conductive parcel is presented and used to model the electric arc, however the arc current is composed of all the
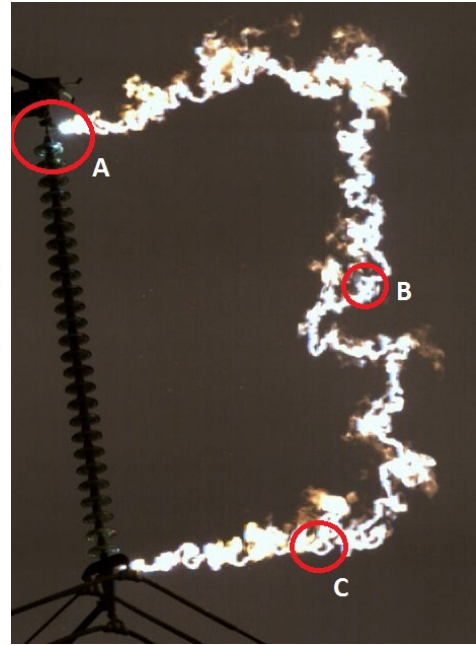

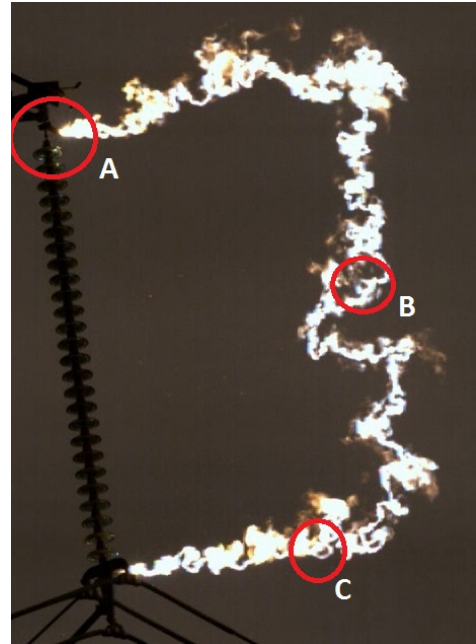Fig. 16: Image detail for a closing loop occurrence.

Fig. 17: Image detail for a closing loop occurrence.

described components, specifically the conductive current, the displacement current and the residual current.

To derive the arc conductance it is necessary to use only the conductive current, which has to be obtained by applying signal processing techniques.

A process to obtain the conductance and the capacitance from the arc current was proposed and applied to 400 artificially generated long electric arcs. It was possible to observe the expected arc voltage-current characteristic, which cannot
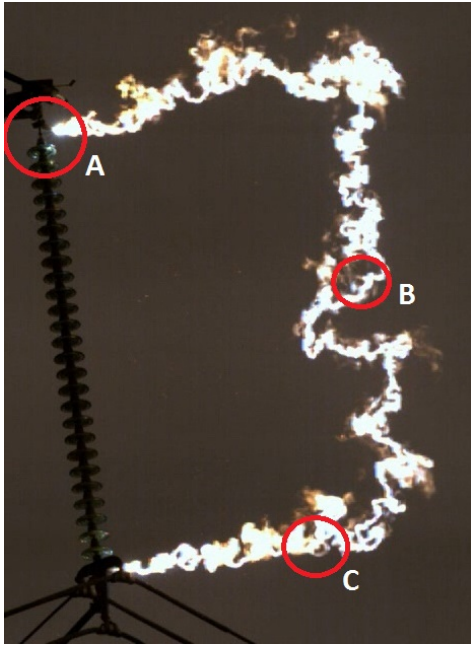
Fig. 18: Image detail for a closing loop occurrence.

be obtained directly from experimental data.

The conductance varied with the arc current level, from 1.3 mS (15 A_{rms}) to 557.58 mS (3000 A_{rms}). Regarding the capacitance, the values varied from 0.62 μF (15 A_{rms}) to 87.71 μF (3000 A_{rms}).

Abrupt changes inside a cycle happens because of the variation of the arc length, caused be closing loops occurrence, and that also changes the pseudo-stationary parameters of the arc.

It is still necessary to extract a per unit value, taking into account the arc length. An ongoing research will present new result in near future.

The conductive arc current can be used to derive the arc model, but the capacitive effect should also be properly represented in the arc model.

ACKNOWLEDGMENT

REFERENCES

[1] M. Djuric and C. Terzija, "A new approach to the arcing faults detection for fast autoreclosure in transmission systems," *IEEE Transactions on Power Delivery*, vol. 10, no. 4, pp. 1793–1798, 1995.

[2] Z. Bo, A. Johns, R. Aggarwal, J. Goody, and B. Gwyn, "Digital simulation of an EHV transmission system for design and real time testing of new protection," in *ICDS '95. First International Conference on Digital Power System Simulators*. IEEE, 1995, p. 57.

[3] A. C. Boisseau, B. W. Wyman, and W. F. Skeats, "Insulator Flashover Deionization Times as a Factor in Applying High-Speed Reclosing Circuit Breakers," *Transactions of the American Institute of Electrical Engineers*, vol. 68, no. 2, pp. 1058–1067, Jul. 1949.

[4] J. Giesbrecht, D. Ouellette, and C. Henville, "Secondary Arc Extinction and Detection Real and Simulated," in *Developments in Power System Protection, 2008. DPSP 2008. IET 9th International Conference on*, 2008, pp. 138 – 143.

[5] R. Luxenburger and P. Schegner, "Determination of secondary arc extinction time and characterization of fault conditions of single-phase autoreclosures," in *2005 International Conference on Future Power Systems*. IEEE, 2005, pp. 5 pp.–5.

[6] K. Milne, "Single-Pole Reclosing Tests on Long 275-Kv Transmission Lines," *IEEE Transactions on Power Apparatus and Systems*, vol. 82, no. 68, pp. 658–661, Oct. 1963.

[7] M. Kizilcay and T. Pniok, "Digital simulation of fault arcs in power systems," *European Transactions on Electrical Power*, vol. 1, no. 1, pp. 55–60, Sep. 1991.

[8] M. Tavares, J. Talaisys, C. Portela, and A. Camara, "Harmonic content and estimation of length variation of artificially generated electrical arc in out-door experiments," in *2011 IEEE Electrical Power and Energy Conference*. IEEE, Oct. 2011, pp. 346–351.

[9] A. S. Câmara, C. M. Portela, and M. C. Tavares, "Single-phase autoreclosure studies considering a robust and reliable secondary arc model based on a gray-box model," in *2008 International Conference on High Voltage Engineering and Application*. IEEE, Nov. 2008, pp. 486–489.

[10] A. S. B. Câmara, C. M. J. C. Portela, and M. C. Tavares, "Single-Phase Auto-Reclosure Studies: Some Basic Aspects on Main Elements Representation," in *2008 International Conference on High Voltage Engineering and Application*. IEEE, Nov. 2008, pp. 482–485.

[11] G. Santos, C. Tozzi, and M. Tavares, "Visual evaluation of the length of artificially generated electrical discharges by 3D-snakes," *IEEE Transactions on Dielectrics and Electrical Insulation*, vol. 18, no. 1, pp. 200–210, Feb. 2011.

[12] Q. Li, H. Cong, Q. Sun, J. Xing, and Q. Chen, "Characteristics of Secondary AC Arc Column Motion Near Power Transmission-Line Insulator String," *IEEE Transactions on Power Delivery*, vol. 29, no. 5, pp. 2324–2331, Oct. 2014.